Ergodic Capacity Analysis for Terrestrial-LEO-GEO Relay Systems With Stochastic Orbit Modeling

Tingting Li, Hui Zhao, Rui Zhang, and Gaofeng Pan

***Abstract*—This paper investigates an uplink transmission from a terrestrial user to a geostationary Earth orbit (GEO) satellite, using multiple low Earth orbit (LEO) satellites as amplify-and-forward (AF) relays. We first model the altitudes of LEO spherical orbits as a one-dimensional stochastic point process, where multiple satellites are randomly and uniformly distributed along each orbit. Then, we derive an approximate expression for the ergodic capacity by introducing a novel stochastic geometry-based analytical approach, which effectively captures the impact of random satellite distributions on system performance. Using this approximation method, we also derive the ergodic capacity accounting for the one-dimensional Poisson point process (PPP) and the terrestrial-satellite channel modelled with Rician-shadowed fading. Finally, the accuracy of the derived expressions is validated through Monte Carlo simulations, and the results further confirm that the one-dimensional PPP can accurately approximate the delivery performance even when a reasonable minimum inter-orbit distance for LEO satellites is considered.**

***Index Terms*—Amplify-and-forward relaying, ergodic capacity, stochastic point process, terrestrial-LEO-GEO system.**

I. Introduction

The rapid development of satellite communication systems has spurred significant interest in hybrid terrestrial-satellite networks, especially those involving low Earth orbit (LEO) satellites [1]–[3]. LEO satellites provide global coverage and low-latency communication, making them suitable for a wide range of applications, including broadband internet services, remote sensing, and disaster management. Meanwhile, geostationary Earth orbit (GEO) satellites remain crucial due to their fixed position relative to the Earth, allowing continuous communication with a large ground area [4]–[6].

Establishing a reliable communication link between terrestrial users and GEO satellites presents significant challenges due to severe pathloss and shadowing effects caused by the long distances and obstructions in the direct line-of-sight (LoS) path. To address these issues, LEO satellites, positioned much closer to the Earth's surface, can serve as relay nodes, facilitating signal transmission between terrestrial users and GEO satellites [7], [8]. However, the studies in [7], [8] considered only a simplified scenario involving a single random LEO satellite as a relay, without accounting for the more realistic and increasingly relevant scenario of multiple LEO satellites acting as relays. This limitation overlooks the potential of utilizing multiple LEO relays, which has become feasible with the rapid expansion of LEO satellite constellations.

Tingting Li is with the School of Mathematics and Statistics, Southwest University, Chongqing, China (email: tinalee@swu.edu.cn).

Hui Zhao is with the Communication Systems Department, EURECOM, 06410 Sophia Antipolis, France (email: hui.zhao@eurecom.fr).

Rui Zhang and Gaofeng Pan are with the School of Cyberspace Science and Technology, Beijing Institute of Technology, Beijing, China (email: rui.zhang@bit.edu.cn; gfpan@bit.edu.cn).

Tingting Li and Hui Zhao contributed equally to this work.

Stochastic geometry (SG) provides a powerful framework for analyzing the performance of complex networks, including satellite communication systems, by modeling the spatial distributions of network components as stochastic point processes [9]. Among the various models, the spherical binomial point process (BPP) is particularly effective for representing scenarios where a finite number of satellites are distributed uniformly on a spherical surface. Although BPP-based models do not fully account for the deterministic structures of actual satellite constellations, prior studies have shown that these differences have minimal impact on network topology and performance metrics [10]. Consequently, the BPP model strikes a balance between analytical tractability and modeling accuracy, making it a practical choice for large-scale satellite networks.

A very recent study [11] adopted the SG framework to model multiple LEO satellites serving as relays for data transmission from a terrestrial user to a GEO satellite. This work modeled LEO satellites as a spherical homogeneous BPP, assuming a uniform distribution within a single spherical orbit. While this approach offers mathematical simplicity, it is limited by its focus on a single LEO orbit, which does not adequately capture the complexity of current and future mega-LEO constellations comprising multiple orbits. Another recent work [12] extended the SG-based analysis to model multiple LEO orbits, providing insights into the communication performance between terrestrial users and LEO satellites. However, this study exclusively focused on terrestrial-to-LEO communications, without considering the uplink transmission to GEO satellites. This omission limits the applicability of its results in scenarios requiring GEO satellites for global coverage and long-distance communication.

Within the SG analytical framework, the ergodic capacity is often derived by integrating the outage probability (OP) expression, which itself may involve complex formulations. These prior studies, including [11] and [12], primarily focus on analyzing OP or its variants, such as the coverage probability, but do not examine the ergodic capacity. However, ergodic capacity is a critical performance metric as it represents the long-term average data transmission rate over varying channel conditions [13, Ch. 4]. Unlike OP, which provides a snapshot view of the system's performance under specific conditions, ergodic capacity captures the system's average delivery performance and reliability over time, making it more relevant for applications requiring consistent communication quality. Despite its importance, calculating ergodic capacity within the SG framework often introduces significant computational challenges due to the additional infinite integral over already complex OP expressions [14]. This underscores the need for a computationally efficient approach to evaluate the ergodic capacity in SG-based analysis.

In this paper, we analyze the delivery performance of an uplink transmission from a terrestrial user to a GEO satellite via multiple LEO relays, where the relays employ the amplify-and-forward (AF) strategy. We first model the altitudes of LEO satellites using a general one-dimensional stochastic point process and assume that a finite number of LEO satellites are uniformly distributed on the spherical surface of each LEO orbit, following a BPP. Based on this model, we derive an approximate expression for the system's ergodic capacity using a novel analytical approach that significantly reduces computational complexity. Building on this, we focus on a specific case where the LEO altitudes are modeled as a one-dimensional homogeneous Poisson point process (HPPP), with the terrestrial-satellite channels subject to Rician-shadowed fading. Using the approximation derived for the general stochastic process case, we further obtain an analytical expression for the ergodic capacity under the HPPP and Rician-shadowed fading assumptions. Finally, we validate the accuracy of the analytical expression for HPPP through Monte Carlo simulations, demonstrating that the HPPP remains robust even when a practical minimum contact distance is enforced between adjacent LEO orbits. This consideration is particularly relevant for real-world satellite deployments and highlights the practical applicability of our framework.

II. System Model

As illustrated in Fig. 1, a terrestrial node (denoted by S) seeks to communicate with a GEO satellite. However, due to significant factors such as long distances and severe obstructions, the direct link between S and the GEO satellite experiences heavy shadowing, leading to unreliable performance. To enhance the uplink communication quality, LEO satellites within the field-of-view (FoV) of S serve as AF relays[1]. These LEO satellites are distributed across various LEO *spherical* orbits at altitudes ranging from H_l to H_u above the Earth's surface. The communication procedure consists of two phases: First, S transmits its signal to both the GEO satellite and the LEO satellites. Due to the heavy shadowing on the direct link, the LEO satellites assist by relaying the received signal from S to the GEO satellite using the AF strategy. Finally, the GEO satellite combines the direct signal (received under heavy shadowing) with the relayed signals from the LEO satellites for decoding.

The altitudes of these LEO spherical orbits can be modelled as a one-dimensional stochastic point process.[2] Similar to [16], [17], we consider that N LEO satellites are uniformly placed on the *sphere's* surface of each LEO orbit. To describe the positions of the communications nodes under consideration, we establish a right-hand Cartesian coordinate system in Fig. 1, with the vertical axis z defined as the line connecting the Earth's center to the terrestrial node S. After that, we use β to denote the zenith angle of the GEO satellite. We use θ_m to define the maximum FoV angle of S. That is, as long as the zenith angle of an LEO satellite *w.r.t.* S lies in the interval $[0, \theta_m]$, we treat it as a feasible relay forwarding the messages of S. Using basic geometric principles, the maximum zenith angle θ_{jm} of a serving LEO satellite located in an orbit with a radius r_j relative to the Earth's center can be easily derived. Specifically, the cosine of θ_{jm} is given by the following expression

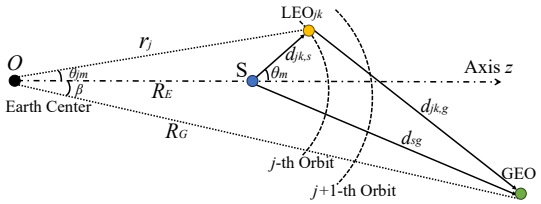

Fig. 1: A two-dimensional cross-sectional view illustrating an LEO satellite at the maximum FoV angle of the land user S in the j-th orbit, serving as a relay for uplink communication from S to the GEO satellite.

$$\cos\theta_{jm} = \sqrt{1 - \frac{1}{r_j^2}\left(\sqrt{r_j^2\sin^2\theta_m - R_E^2\sin^4\theta_m} - R_E\cos\theta_m\sin\theta_m\right)^2} \tag{1}$$

where R_E denotes the radius of the Earth. Based on some basic probability theory, we have the following proposition.

Proposition 1: The number of serving LEO satellites on the j-th orbit with radius r_j, where r_j itself is a random variable, follows a binomial distribution with a success probability of $(1-\cos\theta_{jm})/2$, conditioned on a specific value of r_j.

Proof: This is determined by the ratio of the surface area within the broadcasting region, where the available LEO satellites can reside, to the total surface area of the j-th spherical orbit. This ratio applies because the LEO satellites are assumed to be randomly and uniformly distributed on the spherical surface of their respective orbit. ■

A. Channel Model

We assume that the terrestrial-satellite channel experiences both small-scale fading and pathloss, while the link between any LEO satellite and the GEO satellite is affected only by large-scale pathloss[3]. Small-scale fading in the terrestrial-satellite link is modelled using Rician-shadowed fading. Let LEO$_{jk}$ denote the k-th serving LEO satellite in the j-th orbit, and let h_{jk} represent the small-scale channel gain for the S–LEO$_{jk}$ link. The statistics of h_{jk} are determined by three parameters: m_{se}, b_{se}, and Ω_{se}. Specifically, $2b_{se}$ represents the average power of the scattered component, while Ω_{se} denotes the average power of the LoS component. The parameter m_{se} reflects the obstruction degree of the LoS component. We refer to [18] for

[1]While the studies in [7], [8] utilized the decode-and-forward (DF) scheme, this approach becomes increasingly complex and less practical when massive LEO relays are involved. In contrast, the AF scheme offers a more efficient and scalable alternative for such scenarios. By simply amplifying and forwarding the received signals without requiring decoding at each relay [15], the AF scheme significantly reduces the processing complexity, making it a more suitable choice for large-scale LEO satellite networks.

[2]While traditional satellite constellations are often characterized by fixed parameters, such as specific altitudes and well-defined orbital planes, LEO satellites are subject to dynamic variations influenced by gravitational perturbations, atmospheric drag, and adjustments from operational maneuvers. As discussed in [12], modeling LEO altitudes using a one-dimensional stochastic point process offers a more adaptive and practical framework to account for these variations and evaluate delivery performance effectively.

[3]The LEO-GEO link is assumed to be dominated by large-scale pathloss only, as it involves a high-altitude satellite-to-satellite connection with clear LoS conditions and minimal scattering or shadowing effects. Given the vast distance and the absence of terrestrial obstacles, small-scale fading is negligible.

more details. The probability density function (PDF) of $|h_{jk}|^2$ is given by [18, Eq. (6)].

$$f_{|h_{jk}|^2}(x) = \alpha_{se} \exp(-\varphi_{se} x)\ {}_1F_1(m_{se}; 1; \delta_{se} x), \quad (2)$$

where $\alpha_{se} \triangleq \frac{1}{2b_{se}} \left(\frac{2b_{se} m_{se}}{2b_{se} m_{se} + \Omega_{se}} \right)^{m_{se}}$, $\varphi_{se} \triangleq \frac{1}{2b_{se}}$, and $\delta_{se} \triangleq \frac{\Omega_{se}}{2b_{se}(2b_{se} m_{se} + \Omega_{se})}$. In (2), ${}_1F_1(\cdot;\cdot;\cdot)$ denotes the confluent Hypergeometric function of the first kind [19]. Similarly, the channel gain from S to the GEO satellite h_{sg} is also characterized by three parameters: m_{sg}, b_{sg} and Ω_{sg}.

B. AF Relaying

The received signal at LEO$_{jk}$ during the first phase is $y_{jk,s} = \sqrt{L_s d_{jk,s}^{-\alpha_1}} h_{jk} s + z_{jk}$, where $s \in \mathbb{C}$ denotes the signal transmitted by S, and L_s denotes the transmit signal-to-noise ratio (SNR) at S, and $d_{jk,s}$ denotes the distance from S to LEO$_{jk}$, and $\alpha_1 > 0$ denotes the pathloss exponent of the terrestrial-LEO satellite channel. z_{jk} denotes the Additive White Gaussian Noise (AWGN) with zero-mean and unit-variance. We assume that the AF gain at each LEO satellite dynamically adjusts to compensate for channel fading in each instantaneous channel realization. To limit the output power of the relay when inverting the channel in deep fading, the AF gain at LEO$_{jk}$ is of the form [15] $A_{jk} = \frac{1}{1+\text{SNR}_{jk,s}} \in [0, 1]$, where $\text{SNR}_{jk,s} \triangleq L_s d_{jk,s}^{-\alpha_1} |h_{jk}|^2$ denotes the received SNR at LEO$_{jk}$. To prevent signal cancellation at the GEO satellite caused by phase differences from multiple relays, each relay applies a phase shift. This phase adjustment is *essential* due to the differing positions of the LEO relays relative to the GEO satellite. Under the AF relaying strategy and the phase shift ϕ_{jk}, the transmit signal at LEO$_{jk}$ takes the form

$$y_{jk,g} = \sqrt{L_r A_{jk}} \exp(\jmath \phi_{jk}) \left(\sqrt{L_s d_{jk,s}^{-\alpha_1}} h_{jk} s + z_{jk} \right), \quad (3)$$

where L_r represents the power applied by LEO$_{jk}$ after inverting the first hop channel.

Again during the first phase, the GEO can also receive the signal sent from the source S, despite the heavy shadowing over the channel. Specifically, the signal received at the GEO satellite during the first phase is given by

$$y_{sg} = \sqrt{L_s d_{sg}^{-\alpha_0}} h_{sg} s + z_{g1}, \quad (4)$$

where d_{sg} and α_0 denote the delivery distance between S and G and the pathloss exponent respectively, and $z_{g1} \sim \mathcal{CN}(0, 1)$ denotes the AWGN at the GEO satellite during the first phase.

Recall that the second hop from the LEO satellite to the GEO satellite only suffers from the large-scale pathloss. We use Φ and $\mathcal{N}_j$ to respectively denote the collection sets of the LEO orbits and the serving LEO satellites in the j-th orbit. The combined signal over the two hops at the GEO satellite is

$$y_g = y_{sg} + \sum_{j \in \Phi} \sum_{k \in \mathcal{N}_j} \sqrt{L_r d_{jk,g}^{-\alpha_2}} y_{jk,g} + z_{g2} \quad (5)$$

where $d_{jk,g}$ denotes the distance from LEO$_{jk}$ to G, and $\alpha_2 > 0$ denotes the pathloss exponent of the LEO-GEO channel, and $z_{g2} \sim \mathcal{CN}(0, 1)$ denotes the AWGN at the GEO satellite during the second hop. After substituting y_{sg} and $y_{jk,g}$ into the above, we can express the combined signal as (6), shown at the top of the next page. To ensure that the signals from multiple LEO relays do not cancel each other out and to prevent the relayed signals from interfering destructively with the direct link signal, we apply the phase shift $\phi_{jk} = -\text{Arg}\{h_{jk}\} - \text{Arg}\{h_{sg}\} + \frac{\pi}{2}$ at LEO$_{jk}$. Here, Arg$\{\cdot\}$ represents the phase of the complex number.[4] The SNR for decoding s at the GEO satellite is expressed as (7), shown at the top of the next page.

The ergodic capacity of this hybrid terrestrial-satellite system is of the form

$$\bar{C} = \frac{1}{2} \mathbb{E} \left\{ \log_2 \left(1 + \text{SNR}_g \right) \right\} \text{ bits/s/Hz} \quad (8)$$

where the ergodic capacity is averaged over small-scale channel fading and random locations of LEO satellites.[5]

III. Performance Analysis

In this section, we first parameterize the ergodic capacity defined in (8) for a general one-dimensional stochastic point process to model the random LEO altitudes. We then focus on the specific case of an HPPP with Rician-shadowed fading channels and derive the corresponding ergodic capacity.

Before the main results, we define the following parameters[6]

$$\Xi_1 \triangleq \mathbb{E} \left\{ \sum_{j \in \Phi} |\mathcal{N}_j|^2 d_{j,g}^{-\alpha_2} \right\} \quad (9)$$

$$\Xi_2 \triangleq \mathbb{E} \left\{ \mathbb{I}\{|\Phi| \geq 2\} \sum_{j \in \Phi} \sum_{i \in \Phi, i \neq j} |\mathcal{N}_j| |\mathcal{N}_i| \sqrt{d_{j,g}^{-\alpha_2} d_{i,g}^{-\alpha_2}} \right\} \quad (10)$$

$$\Xi_3 \triangleq \mathbb{E} \left\{ \sum_{j \in \Phi} \sum_{k \in \mathcal{N}_j} \frac{L_r (R_g^2 + r_j^2 - 2 R_g r_j \cos\beta)^{-\alpha_2/2}}{1 + L_s (r_j - R_e)^{-\alpha_1} |h_{jk}|^2} \right\}, \quad (11)$$

where $\mathbb{I}\{\cdot\}$ denotes the well-known indicator function. $\mathbb{I}\{|\Phi| \geq 2\}$ equals 1 if $|\Phi| \geq 2$; otherwise, it equals 0.

Theorem 1: For any one-dimensional stochastic point process Φ to model the random LEO altitudes and for any fading channels, we can always approximate the ergodic capacity of the considered hybrid terrestrial-satellite system as[7] $\bar{C} \approx \frac{1}{2} \log_2 (1 + \bar{\gamma})$, where $\bar{\gamma}$ is defined as

$$\bar{\gamma} \triangleq \frac{L_s d_{sg}^{-\alpha_0} \mathbb{E}\{|h_{sg}|^2\} + L_r \Xi_1 + L_r \Xi_2}{2 + \Xi_3}. \quad (12)$$

Proof: The proof is relegated to Appendix I. ■

[4]The Doppler shift caused by the high-speed movement of LEO satellites introduces additional phase noise and frequency offset, potentially degrading system performance if not properly mitigated. Literature such as [11] discusses techniques like bit synchronization adjustments and spectrum spreading to counter these effects effectively. Additionally, while we assume perfect beam alignment, real-world pointing errors caused by jitter could reduce the received signal power. These effects are typically mitigated in practical systems through advanced tracking and alignment techniques, but a detailed analysis of their impact could serve as an extension of this work.

[5]In this paper, $\mathbb{E}\{\cdot\}$ represents the expectation over all random variables, while $\mathbb{E}_X\{\cdot\}$ indicates the expectation taken only over the random variable X. Additionally, $\mathbb{E}\{\cdot|X\}$ denotes the expectation conditioned on X.

[6]Here, we have a slight abuse of notation where $|\cdot|$ denotes both the cardinality of a set and the magnitude of a complex number.

[7]Terrestrial interference, which can degrade the ergodic capacity in practical systems, was not explicitly analyzed in this work. However, our analytical framework can accommodate such interference by modeling it as additional Gaussian noise in the worst-case scenario, which enhances the overall noise power at the satellites. Consequently, the derived results serve as strict lower bounds for the system's performance when terrestrial interference is present.

$$y_g = \sqrt{L_s d_{sg}^{-\alpha_0}} h_{sg} s + \sum_{j\in\Phi}\sum_{k\in\mathcal{N}_j} \sqrt{L_r L_s d_{jk,s}^{-\alpha_1} d_{jk,g}^{-\alpha_2} A_{jk}} h_{jk} \exp(\jmath\phi_{jk}) s + \sum_{j\in\Phi}\sum_{k\in\mathcal{N}_j} \sqrt{L_r d_{jk,g}^{-\alpha_2} A_{jk}} \exp(\jmath\phi_{jk}) z_{jk} + z_{g1} + z_{g2} \quad (6)$$

$$\mathrm{SNR}_g = \frac{\left| \sqrt{L_s d_{sg}^{-\alpha_0}} h_{sg} + \sum_{j\in\Phi}\sum_{k\in\mathcal{N}_j} \sqrt{L_r L_s d_{jk,s}^{-\alpha_1} d_{jk,g}^{-\alpha_2} A_{jk}} h_{jk} \exp\left(-\jmath\mathrm{Arg}\{h_{jk}\} - \jmath\mathrm{Arg}\{h_{sg}\} + \jmath\frac{\pi}{2}\right)\right|^2}{2 + \sum_{j\in\Phi}\sum_{k\in\mathcal{N}_j} L_r d_{jk,g}^{-\alpha_2} A_{jk}} \quad (7)$$

$$\Xi_1 = \lambda \int_{H_l+R_E}^{H_u+R_E} \left(N^2 \frac{(1-\cos\theta_{jm})^2}{4} + N\frac{(1-\cos^2\theta_{jm})}{4} \right) (R_g^2 + r_j^2 - 2R_g r_j \cos\beta)^{-\alpha_2/2} \mathrm{d}r_j \quad (13)$$

$$\Xi_2 = \left(\lambda \int_{H_l+R_\mathrm{E}}^{H_u+R_\mathrm{E}} N\frac{1-\cos\theta_{jm}}{2} (R_g^2 + r_j^2 - 2R_g r_j \cos\beta)^{-\alpha_2/4} \mathrm{d}r_j \right)^2 \quad (14)$$

$$\Xi_3 = L_r \lambda \int_{H_l+R_E}^{H_u+R_E} \frac{N(1-\cos\theta_{jm})}{2(R_g^2 + r_j^2 - 2R_g r_j \cos\beta)^{\alpha_2/2}} \int_0^\infty \frac{\alpha_{se} \exp(-\varphi_{se} x)\ {}_1F_1(m_{se}; 1; \delta_{se} x)}{1 + L_s (r_j - R_e)^{-\alpha_1} x} \mathrm{d}x \mathrm{d}r_j \quad (15)$$

In the following, we model the random distribution of LEO altitudes as a one-dimensional HPPP under Rician-shadowed fading channels. Based on Theorem 1, we derive the approximation of the ergodic capacity in Corollary 1.

Corollary 1: For the case of HPPP with intensity λ and Rician-shadowed fading channels, the expectation terms of $\bar{\gamma}$ in (12) are given by (13), (14) and (15), as shown at the top of this page. Additionally, $\mathbb{E}\{|h_{sg}|^2\} = 2b_{sg} + \Omega_{sg}$.

Proof: The proof is relegated to Appendix II. ■

IV. Numerical Results

In this section, we present the numerical analysis of the ergodic capacity for the proposed terrestrial-LEO-GEO relay system. The key simulation parameters are as follows: the radius of the Earth is $R_E = 6371$ km, and the radius of the GEO orbit is $R_G = 42164$ km. The heights of LEO orbits are *uniformly* distributed over the range $[H_l = 160, H_u = 2000]$ km, with an intensity of λ and a minimum contact distance of $c = 50$ km between adjacent LEO orbits. The simulated results, based on the exact SNR in (7), are represented by symbols in Figs. 2–4. For the analytical results, we consider the randomness of LEO altitudes as an HPPP[8] with the same intensity λ and apply Corollary 1 to evaluate the ergodic capacity, depicted as red solid lines in Figs. 2–4. The primary objective of such numerical comparisons is to demonstrate that the simple HPPP model can effectively approximate scenarios where a contact distance constraint is imposed between adjacent LEO orbits. The zenith angle of the GEO satellite is set to $\beta = \frac{\pi}{12}$. For simplification, we assume all pathloss exponents are equal to 2, i.e., $\alpha_0 = \alpha_1 = \alpha_2 = 2$. The terrestrial-GEO link experiences frequent heavy shadowing, while the terrestrial-LEO links experience infrequent light shadowing. As indicated in [18, Table III], the channel parameters for the terrestrial-GEO link are $m_{sg} = 0.739$, $b_{sg} = 0.063$, and $\Omega_{sg} = 8.97 \times 10^{-4}$, while for the terrestrial-LEO link, they are $m_{se} = 19.4$, $b_{se} = 0.158$, and $\Omega_{se} = 1.29$. The total number of satellites in each LEO orbit is $N = 1000$.

In Fig. 2, we analyze the impact of increasing the transmit SNR L_s at the terrestrial user on the ergodic capacity. As L_s increases, the ergodic capacity improves due to the enhanced SNR over both the terrestrial-LEO (first hop) and LEO-GEO (second hop) links. This is expected because stronger signals result in better overall system performance. Moreover, the ergodic capacity increases with the maximum FoV angle θ_m. A larger θ_m allows the terrestrial user to access more LEO satellites, enabling more satellites to act as AF relays. These additional relays improve the overall received power at the GEO satellite, thus enhancing the system performance. The analytical results for the one-dimensional HPPP closely match the simulated results across various θ_m values, confirming its accuracy even when a contact distance constraint is imposed.

Fig. 3 explores the ergodic capacity for varying intensities λ of LEO orbits. As λ increases, more LEO satellites become available to serve as AF relays, resulting in higher ergodic capacity. However, as the intensity λ increases, we observe a slight degradation in the match between the analytical and simulated results. This is particularly noticeable at $\lambda = 0.02$, which corresponds to 20 LEO orbits over 1000 km on average. This value represents the largest LEO orbit intensity, given the minimum contact distance of $c = 50$ km between adjacent LEO orbits. Despite this slight degradation, the one-dimensional HPPP model still provides high accuracy, even under the most challenging case of high orbit intensity.

In Fig. 4, we examine the ergodic capacity when L_r at the LEO satellites is fixed. Unlike Fig. 2, where L_r scales with L_s, the ergodic capacity remains unchanged at low values of L_s. This occurs because the LEO satellites employ AF relaying, where they invert the power sent from the terrestrial user before forwarding the signal to the GEO satellite. In this low L_s regime, the contribution of the direct S–GEO link is negligible, and thus increasing L_s does not significantly affect the end-to-end performance. When L_s is sufficiently large, the direct S–GEO link becomes dominant, resulting in the ergodic capacity converging across different values of L_r. This indicates that at high L_s, the system's performance is primarily

[8]We also adopt the BPP to model LEO deployment, where the number of LEO orbits follows a binomial distribution, in contrast to the Poisson distribution in PPP. As the intensity of LEO orbits increases, the performance difference between BPP and PPP becomes negligible. However, the corresponding numerical comparison is omitted here due to space limitations.

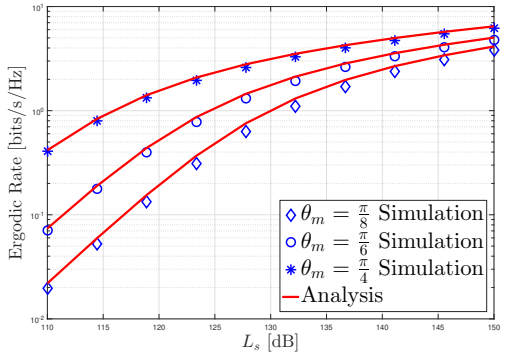

Fig. 2: Ergodic rate versus L_s for $L_r = 2L_s$ and $\lambda = 0.01$ orbits/km

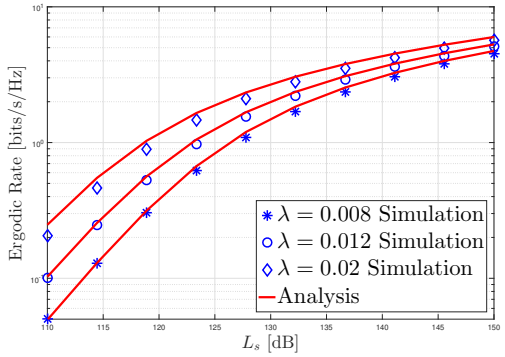

Fig. 3: Ergodic rate versus L_s for $\theta_m = \frac{\pi}{6}$ and $L_r = 2L_s$

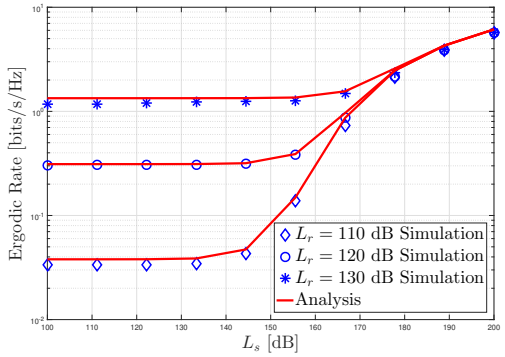

Fig. 4: Ergodic rate versus L_s for $\theta_m = \frac{\pi}{6}$ and $\lambda = 0.01$ orbits/km

influenced by the direct link rather than the relayed links.

V. Conclusions

In this paper, we analyzed the uplink communication from a terrestrial user to a GEO satellite, with multiple LEO satellites acting as AF relays. We first modelled the LEO altitudes using a general one-dimensional stochastic point process and derived an approximate expression for the ergodic capacity. We then considered a special case of HPPP and Rician-Shadowed fading channels, obtaining the corresponding ergodic capacity. The derived results were validated through Monte Carlo simulations, demonstrating a close match between the analytical and simulated results, even when a practical minimum contact distance was enforced between adjacent LEO orbits. These findings confirm the accuracy and effectiveness of using a one-dimensional HPPP to represent the random altitudes of LEO orbits, providing a realistic and practical tool for evaluating performance in LEO-involved satellite systems.

Despite the progress made, several practical factors remain to be addressed. For instance, the treatment of terrestrial interference at the satellites and the potential beam misalignment between satellites can significantly impact the overall delivery performance of the terrestrial–LEO–GEO system. Although terrestrial interference could be modeled as additional Gaussian noise to obtain a tractable lower bound for ergodic capacity, a more comprehensive analysis remains an open challenge. Furthermore, since the adopted spherical BPP framework is also capable of representing the random deployment of UAVs, extending the current study to encompass hybrid aerial networks — such as coordinated UAV-LEO-GEO systems — offers a promising avenue for future research.

Appendix I: Proof of Theorem 1

As suggested in [15], we approximate the AF gain as $A_{jk} \approx \text{SNR}_{jk,s}^{-1} = (L_s d_{jk,s}^{-\alpha_1} |h_{sg}|^2)^{-1}$, which provides a tight approximation to the delivery performance. Substituting this approximate AF gain into (7) and considering the phase shift at each LEO relay, we can simplify the combined SNR as

$$\text{SNR}_g \approx \frac{L_s d_{sg}^{-\alpha_0} |h_{sg}|^2 + \left| \sum_{j\in\Phi} \sum_{k\in\mathcal{N}_j} \sqrt{L_r d_{jk,g}^{-\alpha_2}} \right|^2}{2 + \sum_{j\in\Phi} \sum_{k\in\mathcal{N}_j} L_r d_{jk,g}^{-\alpha_2} A_{jk}}. \quad (16)$$

Based on the SNR approximation in (16) and using [20, Lem. 1], we can approximate the ergodic rate as $\bar{C} \approx \frac{1}{2} \log_2 (1 + \bar{\gamma}')$ where $\bar{\gamma}'$ is defined as

$$\bar{\gamma}' = \frac{\mathbb{E}\left\{ L_s d_{sg}^{-\alpha_0} |h_{sg}|^2 + \left| \sum_{j\in\Phi} \sum_{k\in\mathcal{N}_j} \sqrt{L_r d_{jk,g}^{-\alpha_2}} \right|^2 \right\}}{2 + \mathbb{E}\left\{ \sum_{j\in\Phi} \sum_{k\in\mathcal{N}_j} L_r d_{jk,g}^{-\alpha_2} A_{jk} \right\}}. \quad (17)$$

We note that this approximation becomes tight as the summation terms both in the numerator and the denominator of $\bar{\gamma}'$ increase (cf. [20], [21]). To the best of the authors' knowledge, this approximation method is applied to the analysis of stochastic point processes *for the first time*, though it originates from the analysis in massive multiple-input and multiple-output (MIMO) systems.

For the numerator in (17), we have that

$$\begin{aligned}
&\mathbb{E}\left\{ L_s d_{sg}^{-\alpha_0} |h_{sg}|^2 + \left| \sum_{j\in\Phi} \sum_{k\in\mathcal{N}_j} \sqrt{L_r d_{jk,g}^{-\alpha_2}} \right|^2 \right\} \\
&= L_s d_{sg}^{-\alpha_0} \mathbb{E}\{|h_{sg}|^2\} + \mathbb{E}\left\{ \left| \sum_{j\in\Phi} \sum_{k\in\mathcal{N}_j} \sqrt{L_r d_{jk,g}^{-\alpha_2}} \right|^2 \right\} \\
&\overset{(a)}{\approx} L_s d_{sg}^{-\alpha_0} \mathbb{E}\{|h_{sg}|^2\} + \mathbb{E}\left\{ L_r \left| \sum_{j\in\Phi} |\mathcal{N}_j| \sqrt{d_{j,g}^{-\alpha_2}} \right|^2 \right\} \\
&= L_s d_{sg}^{-\alpha_0} \mathbb{E}\{|h_{sg}|^2\} + L_r \mathbb{E}\left\{ \sum_{j\in\Phi} \sum_{i\in\Phi} |\mathcal{N}_j| |\mathcal{N}_i| \sqrt{d_{j,g}^{-\alpha_2} d_{i,g}^{-\alpha_2}} \right\} \\
&= L_s d_{sg}^{-\alpha_0} \mathbb{E}\{|h_{sg}|^2\} + L_r \Xi_1 + L_r \Xi_2, \quad (18)
\end{aligned}$$

where (a) follows from that we assume the distances from all serving LEO satellites in a given orbit to the GEO satellite are nearly identical, by considering $\cos\theta_{jm} \to 1$. For instance, if we take $\theta_m = \frac{\pi}{6}$ and $r_j = \frac{4}{3} R_E$ (the maximum LEO orbit radius), then using (1), we find that $\cos\theta_{jm} \approx 0.990$.

$$\Xi_3=\mathbb{E}\{|\Phi|\}\mathbb{E}\Big\{\sum_{k\in\mathcal{N}_j}\frac{L_r(R_g^2+r_j^2-2R_gr_j\cos\beta)^{-\alpha_2/2}}{1+L_s(r_j-R_e)^{-\alpha_1}|h_{jk}|^2}\Big\}=\lambda\Delta_H\mathbb{E}\Big\{\frac{N(1-\cos\theta_{jm})}{2}\mathbb{E}_h\Big\{\frac{L_r(R_g^2+r_j^2-2R_gr_j\cos\beta)^{-\alpha_2/2}}{1+L_s(r_j-R_e)^{-\alpha_1}|h_{jk}|^2}\Big\}\Big\} \quad (26)$$

For the denominator of $\bar{\gamma}$ in (17), by using $d_{jk,g}\approx d_{j,g}=\sqrt{R_g^2+r_j^2-2R_gr_j\cos\beta}$, we have that

$$\mathbb{E}\Big\{\sum_{j\in\Phi}\sum_{k\in\mathcal{N}_j}L_{jk}d_{jk,g}^{-\alpha_2}A_{jk}\Big\}\approx\Xi_3. \quad (19)$$

Substituting (18) and (19) into (17), we can derive (12).

Appendix II: Proof of Corollary 1

We use the one-dimensional HPPP with intensity λ to model the radius of the LEO orbits, so the PDF of r_j is given by

$$f_{r_j}(x)=\frac{1}{\Delta_H},\ \text{for } r_j\in[H_l+R_E,H_u+R_E] \quad (20)$$

where $\Delta_H=H_u-H_l$ denotes the length of LEO orbits.

The main derivation of Corollary 1 is to calculate Ξ_1, Ξ_2 and Ξ_3 in Theorem 1 for HPPP and Rician-Shadowed fading channels. In an HPPP, we have the facts: $i)$ the number of LEO orbits $|\Psi|$ and the radius of an arbitrary LEO orbit r_j are independent; $ii)$ $|\mathcal{N}_j|$ and $d_{j,g}$ are independent given r_j; $iii)$ $|\mathcal{N}_j|$ and $|\Psi|$ are independent; $iv)$ $|\Psi|$ follows from a Poisson distribution with the mean of $\lambda\Delta_H$. So we can write Ξ_1 as

$$\begin{aligned}\Xi_1&=\mathbb{E}_\Psi\Big\{\sum\nolimits_{j\in\Phi}\mathbb{E}\{|\mathcal{N}_j|^2|\Psi\}d_{j,g}^{-\alpha_2}\Big\} \quad (21)\\&\overset{(a)}{=}\mathbb{E}_\Psi\Big\{\sum_{j\in\Phi}\Big(N^2\frac{(1-\cos\theta_{jm})^2}{4}+N\frac{(1-\cos^2\theta_{jm})}{4}\Big)d_{j,g}^{-\alpha_2}\Big\}\\&=\mathbb{E}\{|\Psi|\}\mathbb{E}\Big\{\Big(N^2\frac{(1-\cos\theta_{jm})^2}{4}+N\frac{(1-\cos^2\theta_{jm})}{4}\Big)d_{j,g}^{-\alpha_2}\Big\},\end{aligned}$$

where (a) is due to the fact that $|\mathcal{N}_j|$ follows from a Binomial distribution with the success probability of $(1-\cos\theta_{jm})/2$ (cf. Proposition 1). Considering that $\mathbb{E}\{|\Psi|\}=\lambda\Delta_H$ and substituting the PDF of r_j into the above, we can derive (13).

For Ξ_2, considering the facts $i)$, $ii)$ and $iii)$, we have that

$$\begin{aligned}\Xi_2&=\mathbb{E}_\Psi\left\{\mathbb{I}\{|\Phi|\geq2\}|\Phi|(|\Phi|-1)\mathbb{E}^2\left\{|\mathcal{N}_j|d_{j,g}^{-\alpha_2/2}\middle|\Psi\right\}\right\}\\&=\mathbb{E}\{\mathbb{I}\{|\Phi|\geq2\}|\Phi|(|\Phi|-1)\}\,\mathbb{E}^2\Big\{\frac{1-\cos\theta_{jm}}{2N^{-1}}d_{j,g}^{-\frac{\alpha_2}{2}}\Big\}. \quad (22)\end{aligned}$$

Considering the fact $iv)$, we have that

$$\begin{aligned}&\mathbb{E}\left\{\mathbb{I}\{|\Phi|\geq2\}|\Phi|(|\Phi|-1)\right\}\\&=\sum_{n=2}^{\infty}n(n-1)\Pr\{|\Psi|=n\}=\sum_{n=0}^{\infty}n(n-1)\Pr\{|\Psi|=n\}\\&=\mathbb{E}\{|\Psi|(|\Psi|-1)\}=\mathbb{E}\{|\Psi|^2\}-\mathbb{E}\{|\Psi|\}=\lambda^2\Delta_H^2. \quad (23)\end{aligned}$$

Substituting (23) and the PDF of r_j into (22), we get (14).

For Ξ_3, considering the facts $i)-iv)$, we can easily derive (26), as shown at the top of this page. Substituting the PDF of r_j into (26) yields (15). The derivation of $\mathbb{E}\{|h_{sg}|^2\}$ directly follows from [22, Prop. 5.1].

References

[1] P. Yue, *et al.*, "Low earth orbit satellite security and reliability: Issues, solutions, and the road ahead," *IEEE Commun. Surv. Tutor.*, vol. 25, no. 3, pp. 1604–1652, 2023.

[2] S. Wang, J. Ye, C. Chen, G. Pan, and J. An, "Safeguarding inter-satellite transmissions: A viewpoint from covertness," *IEEE Wireless Commun.*, vol. 32, no. 1, pp. 221–228, Feb. 2025.

[3] G. Pan, J. Ye, J. An, and M.-S. Alouini, "Latency versus reliability in LEO mega-constellations: Terrestrial, aerial, or space relay?" *IEEE Trans. Mob. Comput.*, vol. 22, no. 9, pp. 5330–5345, Sep. 2023.

[4] D.-H. Jung, H. Nam, J. Choi, and D. J. Love, "Modeling and analysis of GEO satellite networks," *IEEE Trans. Wireless Commun.*, vol. 23, no. 11, pp. 16 757–16 770, Nov. 2024.

[5] M. He, H. Zhao, X. Miao, S. Wang and G. Pan, "Secure rate-splitting multiple access transmissions in LMS systems," *IEEE Commun. Lett.*, vol. 28, no. 1, pp. 19–23, Jan. 2024.

[6] H. Zhao, A. Bazco-Nogueras, and P. Elia, "Coded caching in land mobile satellite systems," in *Proc. IEEE Int. Conf. Commun. (ICC)*, May 2022.

[7] X. Lin, H. Zhang, G. Pan, S. Wang, and J. An, "LEO relay-aided GEO satellite-terrestrial transmissions," *IEEE Trans. Veh. Technol.*, vol. 72, no. 12, pp. 16 899–16 904, Dec. 2023.

[8] R. Ge *et al.*, "Performance analysis of cooperative nonorthogonal multiple access scheme in two-layer GEO/LEO satellite network," *IEEE Syst. J.*, vol. 16, no. 2, pp. 2300–2310, Jun. 2022.

[9] R. Wang, M. A. Kishk, and M.-S. Alouini, "Ultra-dense LEO satellite-based communication systems: A novel modeling technique," *IEEE Commun. Mag.*, vol. 60, no. 4, pp. 25–31, Apr. 2022.

[10] N. Okati, T. Riihonen, D. Korpi, I. Angervuori, and R. Wichman, "Downlink coverage and rate analysis of low earth orbit satellite constellations using stochastic geometry," *IEEE Trans. Commun.*, vol. 68, no. 8, pp. 5120–5134, Aug. 2020.

[11] J. Zhou, R. Wang, B. Shihada, and M.-S. Alouini, "End-to-end uplink performance analysis of satellite-based IoT networks: A stochastic geometry approach," *IEEE Open J. Commun. Soc.*, vol. 5, pp. 4036–4045, 2024.

[12] H. Zhang *et al.*, "LEO mega-constellation-terrestrial communications suffering poisson arc hardcore distributed space interference," *IEEE Trans. Wireless Commun.*, to be published. DOI: 10.1109/TWC.2024.3523950.

[13] A. Goldsmith, *Wireless Communications*, 2nd ed. Cambridge University Press, 2020.

[14] H. ElSawy, A. Sultan-Salem, M.-S. Alouini, and M. Z. Win, "Modeling and analysis of cellular networks using stochastic geometry: A tutorial," *IEEE Commun. Surv. Tutor.*, vol. 19, no. 1, pp. 167–203, 2017.

[15] M. O. Hasna and M.-S. Alouini, "End-to-end performance of transmission systems with relays over Rayleigh-fading channels," *IEEE Trans. Wireless Commun.*, vol. 2, no. 6, pp. 1126–1131, Nov. 2003.

[16] A. Talgat, M. A. Kishk, and M.-S. Alouini, "Stochastic geometry-based uplink performance analysis of IoT over LEO satellite communication," *IEEE Trans. Aerosp. Electron. Syst.*, vol. 60, no. 4, pp. 4198–4213, 2024.

[17] R. Wang, A. Talgat, M. A. Kishk, and M.-S. Alouini, "Conditional contact angle distribution in LEO satellite-relayed transmission," *IEEE Commun. Lett.*, vol. 26, no. 11, pp. 2735–2739, Nov. 2022.

[18] A. Abdi, W. C. Lau, M.-S. Alouini, and M. Kaveh, "A new simple model for land mobile satellite channels: First- and second-order statistics," *IEEE Trans. Wireless Commun.*, vol. 2, no. 3, pp. 519–528, May 2003.

[19] I. S. Gradshteyn and I. M. Ryzhik, *Table of integrals, series, and products*, 7th ed. Academic press, 2007.

[20] Q. Zhang, S. Jin, K.-K. Wong, H. Zhu, and M. Matthaiou , "Power scaling of uplink massive MIMO systems with arbitrary-rank channel means," *IEEE J. Sel. Signal Process.*, vol. 8, no. 5, pp. 966–981, 2014.

[21] H. Zhao, A. Bazco-Nogueras, and P. Elia, "Vector coded caching multiplicatively boosts the throughput of realistic downlink systems," *IEEE Trans. Wireless Commun.*, vol. 22, no. 4, pp. 2683–2698, 2023.

[22] H. Zhao, "High performance cache-aided downlink systems: Novel algorithms and analysis," Ph.D. dissertation, Sorbonne University, 2022.